



Application of the Space-Time Conservation Element and Solution Element Method to One-Dimensional Advection-Diffusion Problems

Xiao-Yen Wang
Taitech, Inc., Beavercreek, Ohio

Chuen-Yen Chow
University of Colorado at Boulder, Boulder, Colorado

Sin-Chung Chang
Glenn Research Center, Cleveland, Ohio

The NASA STI Program Office . . . in Profile

Since its founding, NASA has been dedicated to the advancement of aeronautics and space science. The NASA Scientific and Technical Information (STI) Program Office plays a key part in helping NASA maintain this important role.

The NASA STI Program Office is operated by Langley Research Center, the Lead Center for NASA's scientific and technical information. The NASA STI Program Office provides access to the NASA STI Database, the largest collection of aeronautical and space science STI in the world. The Program Office is also NASA's institutional mechanism for disseminating the results of its research and development activities. These results are published by NASA in the NASA STI Report Series, which includes the following report types:

- **TECHNICAL PUBLICATION.** Reports of completed research or a major significant phase of research that present the results of NASA programs and include extensive data or theoretical analysis. Includes compilations of significant scientific and technical data and information deemed to be of continuing reference value. NASA's counterpart of peer-reviewed formal professional papers but has less stringent limitations on manuscript length and extent of graphic presentations.
- **TECHNICAL MEMORANDUM.** Scientific and technical findings that are preliminary or of specialized interest, e.g., quick release reports, working papers, and bibliographies that contain minimal annotation. Does not contain extensive analysis.
- **CONTRACTOR REPORT.** Scientific and technical findings by NASA-sponsored contractors and grantees.

- **CONFERENCE PUBLICATION.** Collected papers from scientific and technical conferences, symposia, seminars, or other meetings sponsored or cosponsored by NASA.
- **SPECIAL PUBLICATION.** Scientific, technical, or historical information from NASA programs, projects, and missions, often concerned with subjects having substantial public interest.
- **TECHNICAL TRANSLATION.** English-language translations of foreign scientific and technical material pertinent to NASA's mission.

Specialized services that complement the STI Program Office's diverse offerings include creating custom thesauri, building customized data bases, organizing and publishing research results . . . even providing videos.

For more information about the NASA STI Program Office, see the following:

- Access the NASA STI Program Home Page at <http://www.sti.nasa.gov>
- E-mail your question via the Internet to help@sti.nasa.gov
- Fax your question to the NASA Access Help Desk at (301) 621-0134
- Telephone the NASA Access Help Desk at (301) 621-0390
- Write to:
NASA Access Help Desk
NASA Center for Aerospace Information
7121 Standard Drive
Hanover, MD 21076

NASA/TM—1999-209068



Application of the Space-Time Conservation Element and Solution Element Method to One-Dimensional Advection-Diffusion Problems

Xiao-Yen Wang
Taitech, Inc., Beavercreek, Ohio

Chuen-Yen Chow
University of Colorado at Boulder, Boulder, Colorado

Sin-Chung Chang
Glenn Research Center, Cleveland, Ohio

National Aeronautics and
Space Administration

Glenn Research Center

April 1999

Acknowledgments

The first author would like to thank Dr. Ray Hixon for providing the exact solution of the last test problem. This work was supported by NASA Glenn Research Center through NASA Contract NAS3-97186.

Available from

NASA Center for Aerospace Information
7121 Standard Drive
Hanover, MD 21076
Price Code: A03

National Technical Information Service
5285 Port Royal Road
Springfield, VA 22100
Price Code: A03

Application of the Space-Time Conservation Element and Solution Element Method to One-dimensional Advection-Diffusion Problems

Xiao-Yen Wang

Taitech Inc., NASA Glenn Research Center
Cleveland, Ohio 44135

Chuen-Yen Chow

Department of Aerospace Engineering Sciences
University of Colorado at Boulder
Boulder, Colorado 80309-0429

and

Sin-Chung Chang

NASA Glenn Research Center
Cleveland, Ohio 44135

Abstract

Test problems are used to examine the performance of several one-dimensional numerical schemes based on the space-time conservation and solution element (CE/SE) method. Investigated in this paper are the CE/SE schemes constructed previously for solving the linear unsteady advection-diffusion equation and the schemes derived here for solving the nonlinear viscous and inviscid Burgers equations. In comparison with the numerical solutions obtained using several traditional finite-difference schemes with similar accuracy, the CE/SE solutions display much lower numerical dissipation and dispersion errors.

1. Introduction

The method of space-time conservation element and solution element (to be abbreviated as CE/SE) is a method recently developed by Chang[1] for solving conservation laws. The concept and methodology in this method are significantly different from those in the well-established traditional methods such as the finite difference, finite volume, finite element and spectral methods. First, the flux is conserved in time and space when they are unified and treated equally. Second, all the dependent variables and their derivatives are considered as individual unknowns to be solved simultaneously at each grid point. And third, the concepts of conservation element and solution element are introduced to enforce both the local and global flux conservation without using interpolation or extrapolation. It has been proven that this method is more accurate than some of the traditional methods. The detailed descriptions can be found in [2] and [3].

Several numerical schemes have been constructed earlier in [2] based on the CE/SE method, one of which is the a - μ scheme for solving the 1-D unsteady advection-diffusion equation. Numerical results computed by the a - μ scheme are compared in [3] with those generated by the MacCormack scheme and the Leapfrog/Dufort-Frankel scheme. The comparison shows that the a - μ scheme is superior to the Leapfrog/Dufort-Frankel scheme in accuracy, and has noticeable advantages over the MacCormack scheme in both accuracy and stability.

Two additional examples are presented first to demonstrate the advantageous behavior of the CE/SE a - μ schemes whose solutions display low numerical dissipation and dispersion errors. Solved in those examples are the 1-D unsteady wave equation of hyperbolic type and the 1-D unsteady diffusion equation of parabolic type using the a - μ scheme with $\mu = 0$ and $a = 0$, respectively. Next, the ν - μ scheme for viscous Burgers equation and the ν - ϵ - α scheme for inviscid Burgers equation are derived here based on the CE/SE method. Three test problems are used to demonstrate the effectiveness of the CE/SE method in solving nonlinear problems.

2. Numerical Schemes

In this section a brief review of the space-time CE/SE a - μ scheme developed in [3] is described first, which is followed by the derivation of two numerical schemes for solving the viscous and inviscid Burgers equations.

2.1. The a - μ Scheme for Advection-Diffusion Equation

Consider the linear 1-D unsteady advection-diffusion equation

$$\frac{\partial u}{\partial t} + a \frac{\partial u}{\partial x} = \mu \frac{\partial^2 u}{\partial x^2} \quad (1.1)$$

where a is the advection speed and μ is the viscosity coefficient, both being constant. In the space-time Euclidean space E_2 , the integral form of (1.1) is

$$\int \int_V (\nabla \cdot \vec{h}) dV = 0 \quad (1.2)$$

where $\vec{h} = (au - \mu \frac{\partial u}{\partial x}, u)$ and V is an arbitrary space-time region in E_2 . By the use of Gauss' divergence theorem, Eq. (1.2) becomes

$$\oint_{S(V)} \vec{h} \cdot d\vec{s} = 0 \quad (1.3)$$

where $S(V)$ is the boundary of region V and $d\vec{s} = \pm(dt, -dx)$ [3, p.14].

The conservation element (CE) and solution element (SE) are the two basic elements to be used in the construction of numerical schemes. Some representative $CE(j, n)$ and $SE(j, n)$ are depicted in Fig. 1. At each mesh point (j, n) , there are two CEs corresponding to two unknowns u_j^n and $(u_x)_j^n$. For any $(x, t) \in SE(j, n)$, $u(x, t)$ and $\vec{h}(x, t)$ are approximated by $u^*(x, t; j, n)$ and $\vec{h}^*(x, t; j, n)$, whose definitions are, respectively,

$$u^*(x, t; j, n) = u_j^n + (u_x)_j^n(x - x_j) + (u_t)_j^n(t - t^n) \quad (1.4)$$

where u_j^n , $(u_x)_j^n$ and $(u_t)_j^n$ are constant in $SE(j, n)$, which is the first-order Taylor series expansion, and

$$\vec{h}^*(x, t; j, n) = \left(au^*(x, t; j, n) - \mu \frac{\partial u^*(x, t; j, n)}{\partial x}, u^*(x, t; j, n) \right) \quad (1.5)$$

The assumption that $u = u^*(x, t; j, n)$ satisfies (1.1) implies

$$(u_t)_j^n = -a(u_x)_j^n \quad (1.6)$$

It can be concluded that there are two unknowns u_j^n and $(u_x)_j^n$ at each mesh point (j, n) .

Considering (1.3) in an arbitrary subset of $CE(j, n)$, be it $CE_+(j, n)$ or $CE_-(j, n)$, the approximation is

$$F_{\pm}(j, n) = \oint_{S(CE_{\pm}(j, n))} \vec{h}^* \cdot d\vec{s} = 0 \quad (1.7)$$

Upon substitution of the flux leaving the boundary of $CE_{\pm}(j, n)$ into Eq. (1.7), we can obtain

$$\begin{aligned} \frac{4}{\Delta x^2} F_{\pm}(j, n) &= \pm \frac{1}{2} \left[(1 - \nu^2 + \xi)(u_x)_j^n + (1 - \nu^2 - \xi)(u_x)_{j\pm 1/2}^{n-1/2} \right] \\ &\quad + \frac{2(1 \mp \nu)}{\Delta x} (u_j^n - u_{j\pm 1/2}^{n-1/2}) = 0 \end{aligned} \quad (1.8)$$

where $\nu = a \frac{\Delta t}{\Delta x}$ and $\xi = \frac{4\mu\Delta t}{(\Delta x)^2}$ are the Courant number and diffusion number, respectively. By adding and subtracting the two equations in (1.8), and for $1 - \nu^2 + \xi \neq$

0, we obtain

$$u_j^n = \frac{1}{2} \left\{ (1 + \nu)u_{j-1/2}^{n-1/2} + (1 - \nu)u_{j+1/2}^{n-1/2} + (1 - \nu^2 - \xi) \frac{\Delta x}{4} \left[(u_x)_{j-1/2}^{n-1/2} - (u_x)_{j+1/2}^{n-1/2} \right] \right\} \quad (1.9)$$

$$(u_x)_j^n = \frac{1}{2(1 - \nu^2 + \xi)} \left\{ (\nu^2 - 1) \frac{4}{\Delta x} (u_{j-1/2}^{n-1/2} - u_{j+1/2}^{n-1/2}) - (1 - \nu^2 - \xi) \left[(1 - \nu)(u_x)_{j-1/2}^{n-1/2} + (1 + \nu)(u_x)_{j+1/2}^{n-1/2} \right] \right\} \quad (1.10)$$

Equations (1.9) and (1.10) are the general form of the a - μ scheme. It is an explicit time marching scheme with second-order accuracy in space and time, whose stability condition is $\nu \leq 1$. Detailed descriptions and analysis can be found in [2] and [3].

2.2. The a Scheme for Unsteady Wave Equation

With $\mu = 0$, Eq. (1.1) reduces to the following unsteady wave equation, which is a first-order hyperbolic partial differential equation:

$$\frac{\partial u}{\partial t} + a \frac{\partial u}{\partial x} = 0 \quad (2.1)$$

The a scheme, which is obtained by setting $\xi = 0$ in Eqs. (1.9) and (1.10), is a scheme without any numerical dissipation. Its accuracy and stability condition are the same as those of the a - μ scheme.

2.3. The μ Scheme for Unsteady Diffusion Equation

On the other hand, with $a = 0$ Eq. (1.1) reduces to an unsteady diffusion equation, which is a second-order parabolic partial differential equation:

$$\frac{\partial u}{\partial t} = \mu \frac{\partial^2 u}{\partial x^2} \quad (3.1)$$

The μ scheme for Eq. (3.1) is deduced from (1.9) and (1.10) by letting $\nu = 0$, which has the following form:

$$u_j^n = \frac{1}{2} \left\{ u_{j-1/2}^{n-1/2} + u_{j+1/2}^{n-1/2} + (1 - \xi) \frac{\Delta x}{4} \left[(u_x)_{j-1/2}^{n-1/2} - (u_x)_{j+1/2}^{n-1/2} \right] \right\} \quad (3.2)$$

$$(u_x)_j^n = \frac{1}{2(1 + \xi)} \left\{ -\frac{4}{\Delta x} (u_{j-1/2}^{n-1/2} - u_{j+1/2}^{n-1/2}) - (1 - \xi) \left[(u_x)_{j-1/2}^{n-1/2} + (u_x)_{j+1/2}^{n-1/2} \right] \right\} \quad (3.3)$$

For the boundary CEs, it is obtained from (1.8) that

$$\frac{1}{2} \left[(1 + \xi)(u_x)_j^n + (1 - \xi)(u_x)_{j+1/2}^{n-1/2} \right] + \frac{2}{\Delta x} (u_j^n - u_{j+1/2}^{n-1/2}) = 0 \quad (3.4)$$

for $CE_+(j, n)$, and

$$-\frac{1}{2} \left[(1 + \xi)(u_x)_j^n + (1 - \xi)(u_x)_{j-1/2}^{n-1/2} \right] + \frac{2}{\Delta x} (u_j^n - u_{j-1/2}^{n-1/2}) = 0 \quad (3.5)$$

for $CE_-(j, n)$. At a boundary point with defined u_j^n , $(u_x)_j^n$ can be computed using either Eq. (3.4) or Eq. (3.5) for the left or right boundary.

Note that in the absence of the Courant number ν , the μ scheme is characterized only by the diffusion number ξ and is unconditionally stable with the same accuracy as the a - μ scheme.

2.4. The ν - μ Scheme for Viscous Burgers Equation

If the constant a in Eq. (1.1) is replaced by u , the resulting equation

$$\frac{\partial u}{\partial t} + u \frac{\partial u}{\partial x} = \mu \frac{\partial^2 u}{\partial x^2} \quad (4.1)$$

is called the viscous Burgers equation, which is a nonlinear unsteady advection-diffusion equation with advection speed u . Its conservative form is

$$\frac{\partial u}{\partial t} + \frac{\partial f}{\partial x} = \mu \frac{\partial^2 u}{\partial x^2} \quad (4.2)$$

where $f = \frac{1}{2}u^2$. The ν - μ scheme for (4.2) is derived in a procedure similar to that for the a - μ scheme. Equations (1.2)–(1.4) are still valid here. Instead of Eqs. (1.5) and (1.6), we define

$$f^*(x, t; j, n) = f_j^n + (f_x)_j^n (x - x_j) + (f_t)_j^n (t - t^n) \quad (4.3)$$

where f_j^n , $(f_x)_j^n$ and $(f_t)_j^n$ are also constant in $SE(j, n)$, being respectively the numerical analogues of f , $\partial f / \partial x$, and $\partial f / \partial t$ at grid point (j, n) , and

$$\vec{h}^*(x, t; j, n) = \left(f^*(x, t; j, n) - \mu \frac{\partial u^*(x, t; j, n)}{\partial x}, u^*(x, t; j, n) \right) \quad (4.4)$$

The equivalent of Eq. (1.6) is

$$(u_t)_j^n = -(f_x)_j^n \quad (4.5)$$

Since $f = \frac{1}{2}u^2$, we have

$$f_j^n = \frac{1}{2} (u_j^n)^2 \quad (4.6)$$

$$(f_t)_j^n = u_j^n (u_t)_j^n \quad (4.7)$$

$$(f_x)_j^n = u_j^n (u_x)_j^n \quad (4.8)$$

Substituting the flux leaving the boundary of $CE_{\pm}(j, n)$ into (1.7) results in

$$\begin{aligned} \frac{4}{\Delta x^2} F_{\pm}(j, n) &= \pm \frac{1}{2} \left\{ (1 + \xi)(u_x)_j^n + (1 - \xi)(u_x)_{j\pm 1/2}^{n-1/2} + \left(\frac{\Delta t}{\Delta x}\right)^2 \left[(f_t)_j^n + (f_t)_{j\pm 1/2}^{n-1/2} \right] \right\} \\ &\quad + \frac{2}{\Delta x} \left[\mp \frac{\Delta t}{\Delta x} (f_j^n - f_{j\pm 1/2}^{n-1/2}) + (u_j^n - u_{j\pm 1/2}^{n-1/2}) \right] = 0 \end{aligned} \quad (4.9)$$

Using Eqs. (4.5)–(4.8), we obtain from (4.9)

$$u_j^n = \frac{1}{2} \left[u_{j-1/2}^{n-1/2} + u_{j+1/2}^{n-1/2} + s_{j-1/2}^{n-1/2} - s_{j+1/2}^{n-1/2} \right] \quad (4.10)$$

and

$$(u_x)_j^n = \frac{2}{\Delta x} (u_{j+1/2}^{n-1/2} - u_{j-1/2}^{n-1/2} - s_{j+1/2}^{n-1/2} - s_{j-1/2}^{n-1/2} + \nu_j^n u_j^n) / (1 + \xi - (\nu_j^n)^2) \quad (4.11)$$

where $\nu_j^n = \frac{\Delta t}{\Delta x} u_j^n$, ξ has the same definition as before, and

$$s_{j\pm 1/2}^{n-1/2} = \frac{\Delta x}{4} \left[1 - \xi - (\nu_{j\pm 1/2}^{n-1/2})^2 \right] (u_x)_{j\pm 1/2}^{n-1/2} + \frac{1}{2} \nu_{j\pm 1/2}^{n-1/2} u_{j\pm 1/2}^{n-1/2} \quad (4.12)$$

For boundary CEs, (4.9) reduces to

$$\begin{aligned} \frac{1}{2} \left\{ \left[1 - (\nu_j^n)^2 + \xi \right] (u_x)_j^n + \left[1 - (\nu_{j+1/2}^{n-1/2})^2 - \xi \right] (u_x)_{j+1/2}^{n-1/2} \right\} \\ + \frac{2}{\Delta x} \left[-\frac{1}{2} (\nu_j^n u_j^n - \nu_{j+1/2}^{n-1/2} u_{j+1/2}^{n-1/2}) + (u_j^n - u_{j+1/2}^{n-1/2}) \right] = 0 \end{aligned} \quad (4.13)$$

for $CE_+(j, n)$, and

$$\begin{aligned} -\frac{1}{2} \left\{ \left[1 - (\nu_j^n)^2 + \xi \right] (u_x)_j^n + \left[1 - (\nu_{j-1/2}^{n-1/2})^2 - \xi \right] (u_x)_{j-1/2}^{n-1/2} \right\} \\ + \frac{2}{\Delta x} \left[\frac{1}{2} (\nu_j^n u_j^n - \nu_{j-1/2}^{n-1/2} u_{j-1/2}^{n-1/2}) + (u_j^n - u_{j-1/2}^{n-1/2}) \right] = 0 \end{aligned} \quad (4.14)$$

for $CE_-(j, n)$. At a boundary points with defined u_j^n , $(u_x)_j^n$ can be computed using either Eq. (4.13) or Eq. (4.14) for the left or right boundary.

Note that the Courant number ν_j^n is no longer a constant. Equations (4.10) and (4.11) are the time-marching ν - μ scheme, which is still second-order accurate in space and time. The stability condition is again Courant number being less than 1, i.e., $|u_{max} \frac{\Delta t}{\Delta x}| \leq 1$, which can be derived by von Neumann's stability analysis.

2.5. The ν - ϵ - α Scheme for Inviscid Burgers Equation

The inviscid Burgers equation in conservative form is deduced by letting $\mu = 0$ in Eq. (4.2),

$$\frac{\partial u}{\partial t} + \frac{\partial f}{\partial x} = 0 \quad (5.1)$$

It is expected that the ν - μ scheme may become unstable as $\mu \rightarrow 0$ from the usual behavior of nonlinear problems. To introduce numerical dissipations for computational stability, the assumption $F_{\pm}(j, n) = 0$ is replaced by

$$F_{\pm}(j, n) = \pm \frac{\epsilon(1 - \nu^2)\Delta x^2}{4} (du_x)_j^n \quad (5.2)$$

where ϵ is a constant for controlling the numerical dissipation and

$$(du_x)_j^n = \frac{1}{2} \left[(u_x)_{j+1/2}^{n-1/2} + (u_x)_{j-1/2}^{n-1/2} \right] - (u_{j+1/2}^{n-1/2} - u_{j-1/2}^{n-1/2})/\Delta x \quad (5.3)$$

Also, the flux \vec{h}^* is assumed to be conserved over CE(j, n), i.e.,

$$F(j, n) = \oint_{S(CE(j,n))} \vec{h}^* \cdot d\vec{s} = 0 \quad (5.4)$$

where $\vec{h}^* = (f^*(x, t; j, n), u^*(x, t; j, n))$.

Then following the same procedure as that in deriving the ν - μ scheme, we finally obtain

$$u_j^n = \frac{1}{2} (u_{j-1/2}^{n-1/2} + u_{j+1/2}^{n-1/2} + \hat{s}_{j-1/2}^{n-1/2} - \hat{s}_{j+1/2}^{n-1/2}) \quad (5.5)$$

where

$$\hat{s}_{j\pm 1/2}^{n-1/2} = \frac{\Delta x}{4} \left[1 - (\nu_{j\pm 1/2}^{n-1/2})^2 \right] (u_x)_{j\pm 1/2}^{n-1/2} + \frac{1}{2} \nu_{j\pm 1/2}^{n-1/2} u_{j\pm 1/2}^{n-1/2} \quad (5.6)$$

and

$$(u_x)_j^n = (u_x^{w_0})_j^n + (2\epsilon - 1)(du_x)_j^n \quad (5.7)$$

in which

$$u_x^{w_0} = W_0 [(u_{x-}), (u_{x+}); \alpha] = \frac{|u_{x+}|^\alpha u_{x-} + |u_{x-}|^\alpha u_{x+}}{|u_{x+}|^\alpha + |u_{x-}|^\alpha} \quad (5.8)$$

with

$$(u_{x\pm})_j^n = \pm \frac{u_{j\pm 1/2}^{n-1/2} + \frac{\Delta t}{2} (u_t)_{j\pm 1/2}^{n-1/2} - u_j^n}{\Delta x/2} \quad (5.9)$$

Note that the indices in Eq. (5.8) are dropped for simplicity. Detailed derivations of (5.7)–(5.9) are referred to [2].

In the ν - ϵ - α scheme, ϵ and α are used to control numerical dissipations, and ν is the Courant number. ν and ϵ are restricted by the stability condition that $\nu \leq 1$ and $0 \leq \epsilon \leq 1$, and α is a positive integer, such as 1 or 2, being used to suppress over- and under-shoots near a discontinuity in the solution. Its accuracy is the same as that of the ν - μ scheme.

3. Test Problems and Discussions

All of the one-dimensional schemes described in the previous section are tested using appropriate model problems. The numerical results are compared with those obtained by some traditional finite-difference methods to examine their accuracy.

3.1. Test of the a Scheme

Consider the first-order wave equation

$$\frac{\partial u}{\partial t} + a \frac{\partial u}{\partial x} = 0$$

where $a = 0.5$ in the domain $-1 \leq x \leq 1$. The initial condition is described as

$$u(x, 0) = \sin(\omega x)$$

where $\omega = \pi$. With periodic boundary conditions imposed at $x = -1$ and $x = 1$, the exact solution is

$$u(x, t) = \sin(\omega(x - at))$$

This problem is solved by using the CE/SE a scheme, Lax-Wendroff scheme, and first-order upwinding scheme, respectively. Different Courant numbers with 50 cells are used for each scheme to see the effect of varying the size of time step. Numerical solutions at $t = 10 = 2.5T$ based on the CE/SE scheme, Lax-wendroff (L-W) scheme, and first-order upwind scheme with $CFL = 0.5$ are shown in the upper frame of Fig. 2 with the exact solution plotted as a solid line, while the corresponding error distributions of the first two schemes are shown in the lower frame of Fig. 2. The error is defined as the difference between the numerical solution and the exact solution. It can be seen that the large numerical dissipation in the upwind scheme causes strong damping of the wave amplitude. From the error distribution, it is concluded that the CE/SE scheme has less error than the L-W scheme of the same order of accuracy. In Fig. 3, the results based on $CFL = 0.954$ show that all of the three schemes have smaller errors for larger Courant numbers. The CE/SE scheme is still the most accurate scheme. To see the effect of numerical errors after a long time convection, the CE/SE and L-W solutions and error distribution at $t = 100 = 25T$ are shown in Figs. 4 and 5 for $CFL = 0.5$ and 0.954 , respectively. For the L-W scheme, a large numerical dispersion error is generated by using a smaller time step size when the wave propagates for a long time. Under the same computational conditions, the CE/SE scheme is still more accurate than the L-W scheme.

3.2. Test of the μ Scheme

The μ scheme is used to solve the unsteady diffusion equation (3.1)

$$\frac{\partial u}{\partial t} = \mu \frac{\partial^2 u}{\partial x^2}$$

which was solved in [4] by using several traditional finite-difference methods.

The initial and boundary conditions are stated as follows:

$$\begin{aligned} t = 0, \quad u = U_0 \quad \text{for} \quad x = 0 \\ u = 0 \quad \text{for} \quad 0 < x \leq h \end{aligned}$$

and

$$\begin{aligned} t > 0, \quad u = U_0 \quad \text{for} \quad x = 0 \\ u = 0 \quad \text{for} \quad x = h \end{aligned}$$

For fair comparisons, the grid size $\Delta x = 0.001m$ and physical parameters

$$U_0 = 40 \text{ m/s}, \quad h = 0.04 \text{ m}, \quad \mu = 2.17 \times 10^{-4} \text{ m}^2/\text{s}$$

that are identical to those adopted in other finite-difference schemes are used here. For the CE/SE scheme, $(u_x)_j^n$ are set as zero in the entire domain at $t = 0$, and $(u_x)_j^n$ at the left and right boundaries are computed using Eqs. (3.4) and (3.5), respectively, in the time marching. Figure 6 shows the numerical solution at several selected time steps computed by the μ scheme with $\Delta t = 0.001\text{s}$. Error comparisons of the μ scheme ($\Delta t = 0.001, 0.002$ and 0.003s) with the Forward-Time Central-Space (FTCS) scheme ($\Delta t = 0.002\text{s}$) and Dufort-Frankel (D-F) scheme ($\Delta t = 0.003\text{s}$) are shown in Fig. 7 at $t = 0.18\text{s}$, and in Fig. 8 at $t = 1.08\text{s}$. It is known that relatively large time steps are allowed in both μ scheme and D-F scheme because they are unconditionally stable, whereas the time step size in FTCS scheme is restricted by its stability condition that $\mu \frac{\Delta t}{(\Delta x)^2} \leq \frac{1}{2}$. The comparisons show that the μ scheme is better than the FTCS explicit scheme in both accuracy and stability as time increases, and its performance is generally much better than that of the D-F explicit scheme. Furthermore, the accuracy of the μ scheme increases with decreasing time step.

The Crank-Nicolson implicit scheme was also used to solve the same problem and was found to have generated a highly accurate solution with $\Delta t = 0.01\text{s}$ as shown in [4]. The μ scheme, however, cannot produce solutions of comparable accuracy even with much smaller time step sizes. This fact implies that, in order to improve the accuracy of the μ scheme in the space-time CE/SE method for solving the unsteady diffusion equation, the development of an implicit scheme is needed.

3.3 Test of the ν - μ Scheme

The non-dimensional form of the viscous Burgers equation (3.2) is

$$\frac{\partial u}{\partial t} + \frac{\partial f}{\partial x} = \frac{\partial^2 u}{\partial x^2}$$

which has an analytical solution

$$u = -\frac{2 \sinh x}{\cosh x - e^{-t}}$$

This problem was solved in [4] in the interval $[-9, 9]$ by several finite-difference schemes, such as the FTCS, Dufort-Frankel explicit schemes, and Backward-Time Central-Space (BTCS) implicit scheme. The initial condition for the present numerical computation is set as the analytical solution at $t = 0.1$. The boundary condition is specified as $u = 2.0$ and -2.0 at $x = -9$ and 9 , respectively, and $(u_x)_j^n = 0$ at both boundaries. The grid size $\Delta x = 0.2$ and time step $\Delta t = 0.01$ used here are the same as those in [4]. The numerical solutions at different time levels obtained by the ν - μ scheme with $\Delta t = 0.01$ are plotted in the upper one of Fig. 9 in comparison with the exact solutions plotted as solid lines. The corresponding error profiles are plotted in the lower frame of Fig. 9. Under exactly the same computational conditions, the result of the ν - μ scheme is much more accurate than those computed by the three finite-difference schemes mentioned above, as shown in Fig. 10. For example, at $t = 0.4$ and 1.0 , the maximum errors for the ν - μ scheme are 0.0155 and 6.266×10^{-3} , respectively, as compared to 0.08 and 0.02 for the other three schemes. Keeping the same grid size of $\Delta x = 0.2$, accuracy of the ν - μ scheme can be improved by reducing the time step size as shown in Fig. 11.

3.4. Test of the ν - ϵ - α Scheme

For the inviscid Burgers equation, consider a discontinuous initial condition described by

$$\begin{aligned} u(x, 0) &= 1, & 0.0 \leq x \leq 2.0 \\ u(x, 0) &= 0, & 2.0 \leq x \leq 4.0 \end{aligned}$$

as the first test problem.

Several finite-difference schemes, including Lax, Lax-Wendroff, MacCormack explicit, and Beam-Warming implicit schemes, were used to solve this problem with $\Delta t = 0.1$ and $\Delta x = 0.1$ in [4]. The numerical results obtained by using the ν - ϵ - α scheme with $\epsilon = 0.5$ and $\alpha = 1$ at different times are shown in Fig. 12, disclosing the desired performance in a numerical solution. Unlike the other four schemes, whose results at $t = 0.6$ are shown in Fig. 13, the ν - ϵ - α scheme is able to generate a smooth solution without any oscillations and capture a discontinuity within only two grid points. Figure 14 shows how the time step size affects the solution. The smear of discontinuity is suppressed by increasing Δt or the Courant number ν . The best result is obtained for $\nu_{max} = 1.0$.

The second test problem is taken from [5]. The initial condition is described as

$$u(x, 0) = 0.75 + 0.25 \sin(2\pi x), \quad 0 \leq x \leq 1$$

which is a continuous linear wave. The periodic boundary condition is imposed at $x = 0$ and $x = 1$. The exact solution is referred to [5]. The CE/SE solutions obtained at different time levels using $\Delta x = 0.02$ and $\Delta t = 0.016$ are shown in Fig. 15 in comparison with the exact solution plotted as a solid line. In the upper and lower

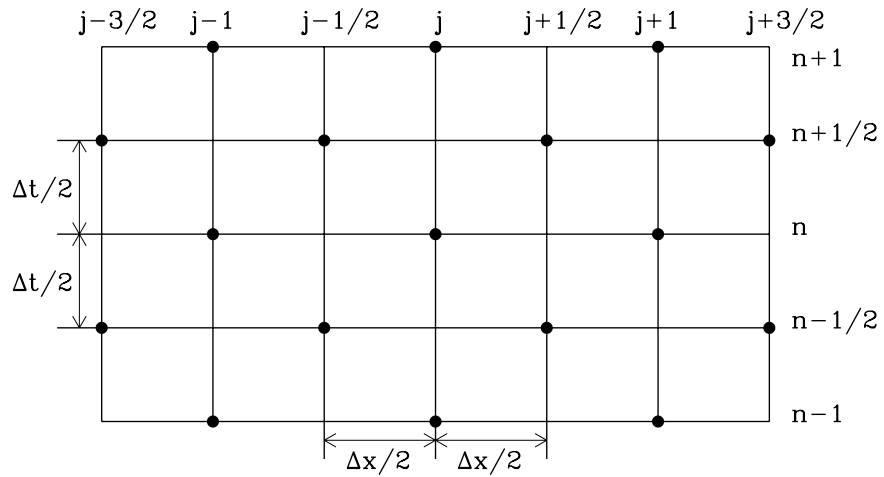
frames of Fig. 15, the solutions at $t = 0.2, 0.4, 0.6$ using $\epsilon = 0, \alpha = 0$, and those at $t = 0.8, 1.0, 1.2, 1.4, 1.6$ using $\epsilon = 0.5, \alpha = 2$, are shown respectively. It can be said that a fairly accurate solution is obtained, especially at later time levels without showing any wiggles near the discontinuity.

Conclusion

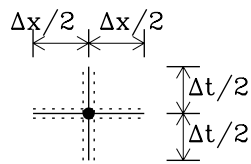
The various schemes based on the space-time conservation element and solution element method have been used to solve the 1-D unsteady wave equation, unsteady diffusion equation, viscous and inviscid Burgers equations. Five numerical test problems have been presented to demonstrate that CE/SE schemes have much lower numerical dissipation and dispersion errors, thus are more accurate than some of the traditional finite-difference methods.

References

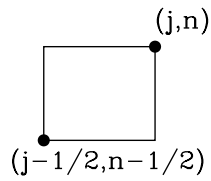
- [1]. Chang, S.C., "The Method of Space-Time Conservation Element and Solution Element – A New Approach for Solving the Navier-Stokes and Euler Equations", *J. Comput. Phys.*, **119**, pp. 295-324, (1995).
- [2]. Chang, S.C., "New Developments in the Method of Space-Time Conservation Element and Solution Element—Applications to the Euler and Navier-Stokes Equations," NASA TM 106226, August, 1993.
- [3]. Chang, S.C. and To, W.M., "A New Numerical Framework for Solving Conservation Laws—The Method of Space-Time Conservation Element and Solution Element," NASA TM 104495, August, 1991.
- [4]. Hoffmann, K. A. and Chiang, S. T., *Computational Fluid Dynamics for Engineers, Vol.I*, Engineering Education System, Wichita, Kansas, 1993.
- [5]. Hixon, R., "Nonlinear Comparison of High-Order and Optimized Finite-difference Schemes," AIAA 98-3240.



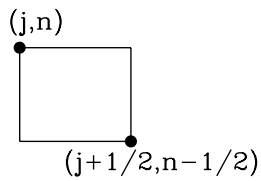
(a) Relative positions of SEs and CEs



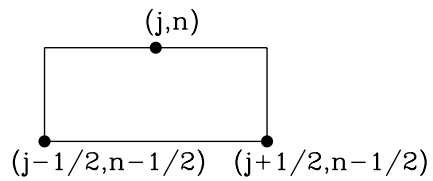
(b) SE(j,n)



(c) CE₋(j,n)



(d) CE₊(j,n)



(e) Interior CE(j,n)

Figure 1: The 1-D CEs and SEs used in the space-time CE/SE method.

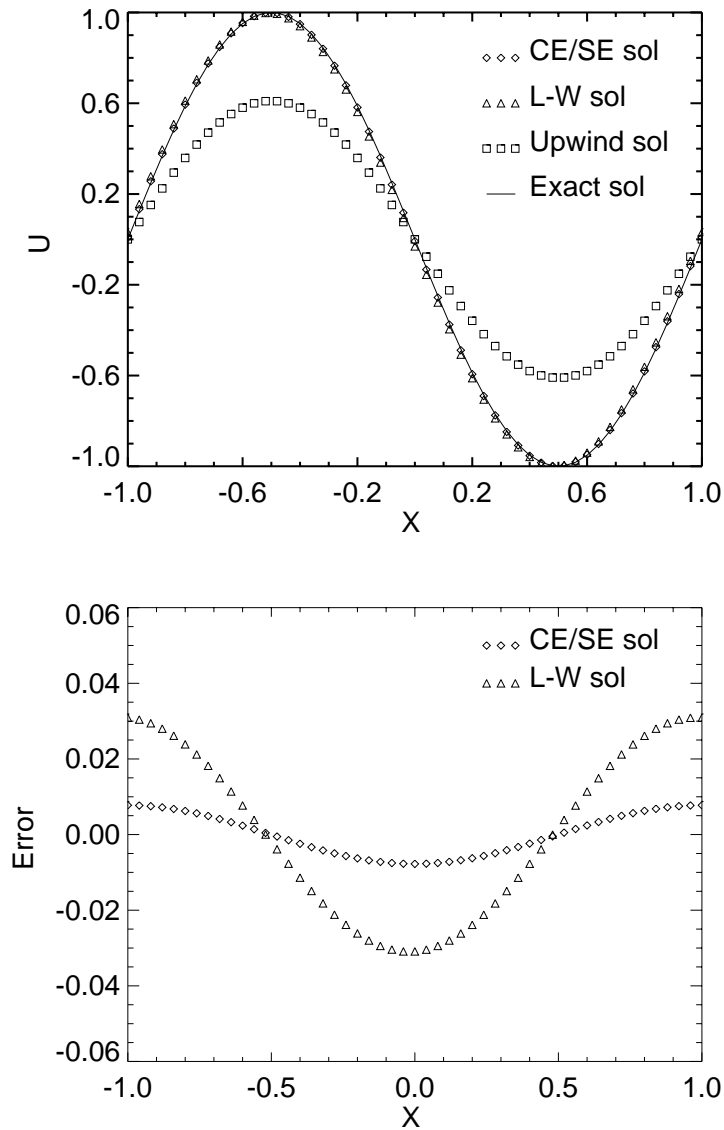


Figure 2: Numerical solutions and the corresponding error distributions at $t = 10$ using $CFL = 0.5$ for various schemes.

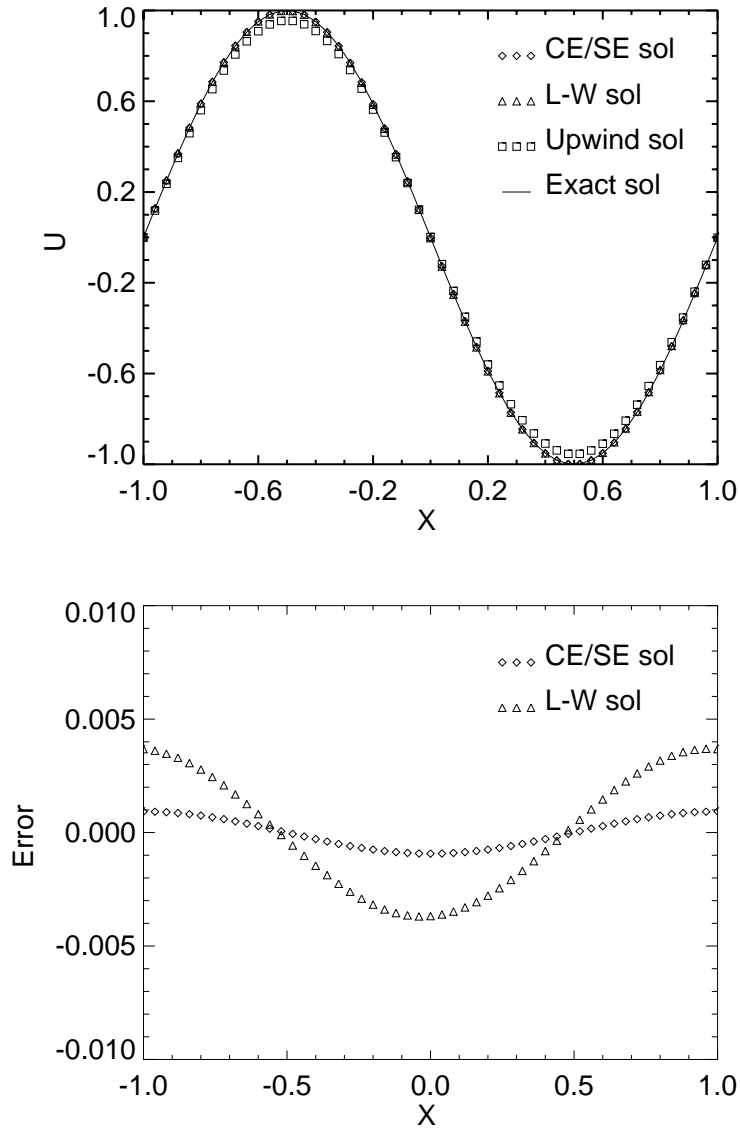


Figure 3: Numerical solutions and the corresponding error distribution at $t = 10$ using $CFL = 0.954$ for various schemes.

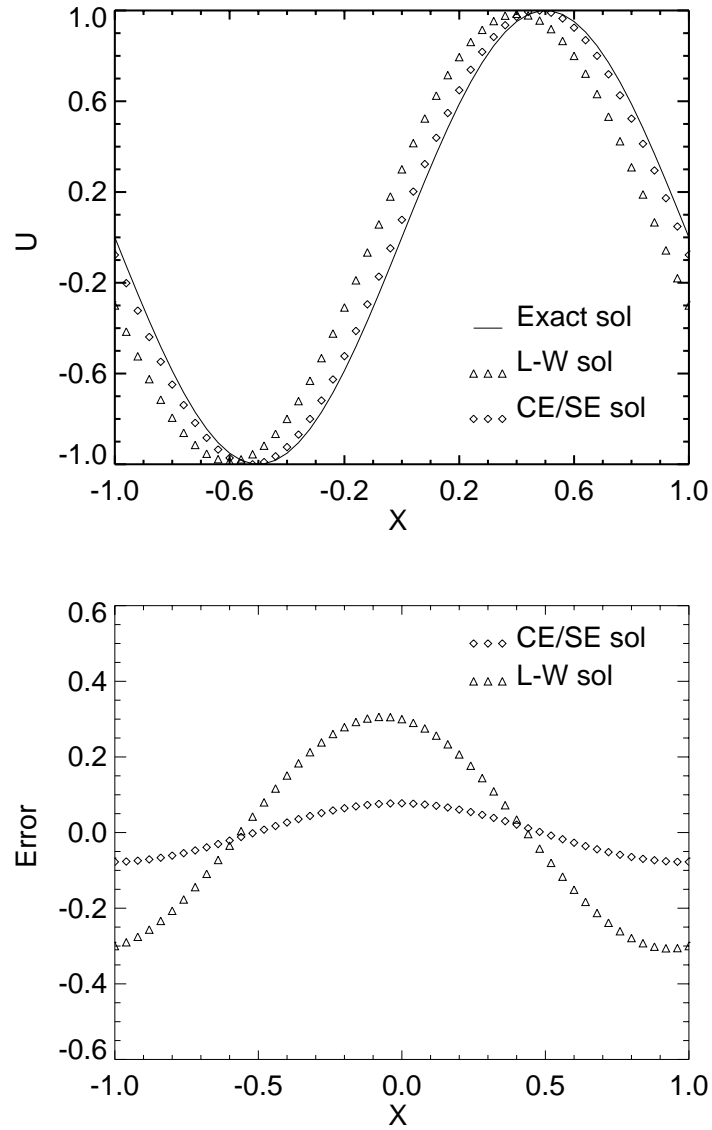


Figure 4: Numerical solutions and the corresponding error distribution at $t = 100$ using $CFL = 0.5$ for various schemes.

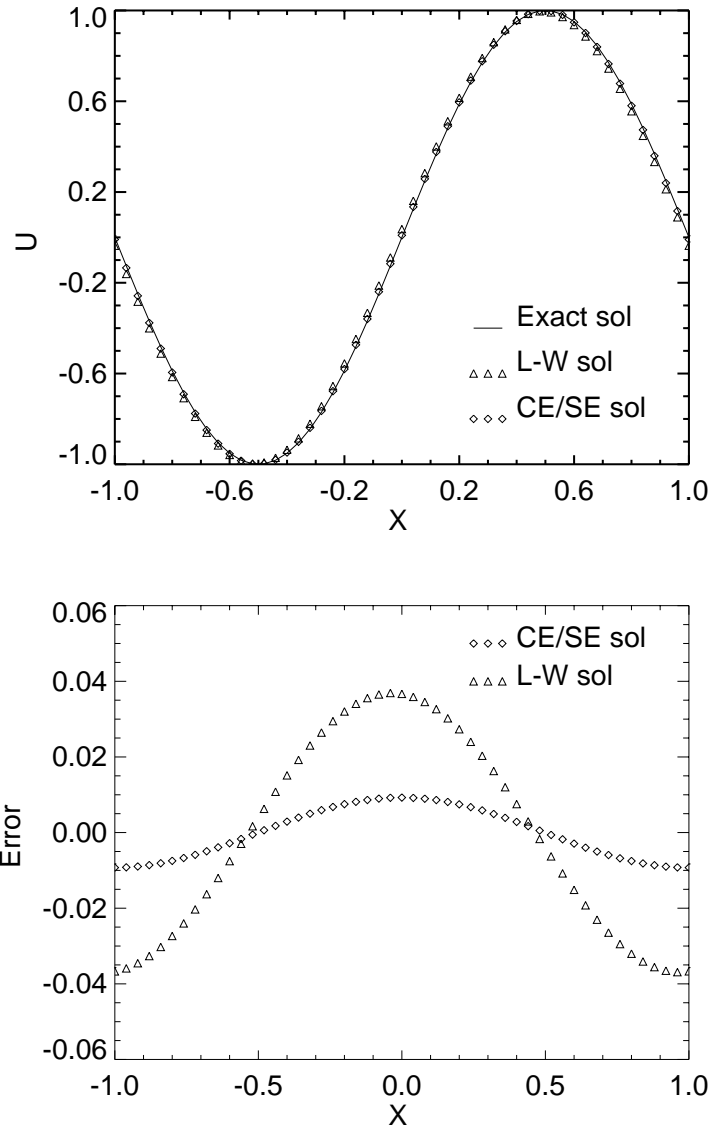


Figure 5: Numerical solutions and the corresponding error distribution at $t = 100$ using $CFL = 0.954$ for various schemes.

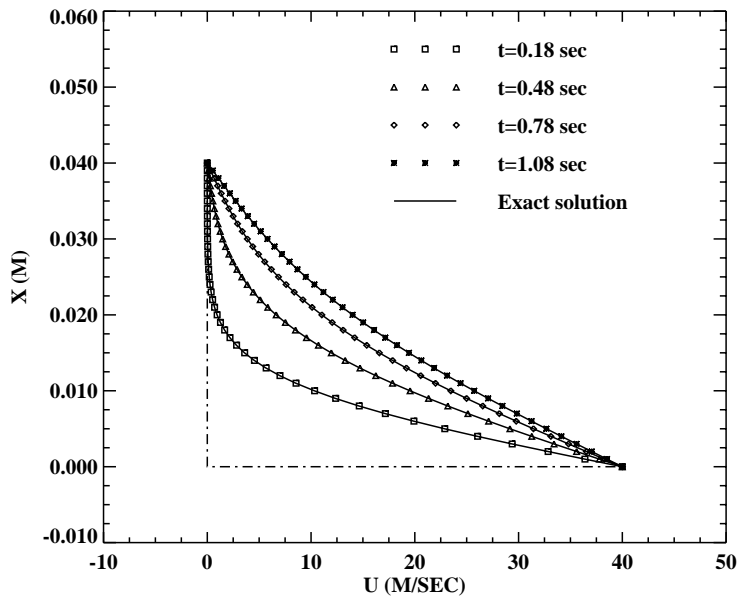


Figure 6: Velocity profiles obtained by the μ scheme ($\xi = 0.868$, $\Delta x = 0.001\text{m}$, $\Delta t = 0.001\text{s}$).

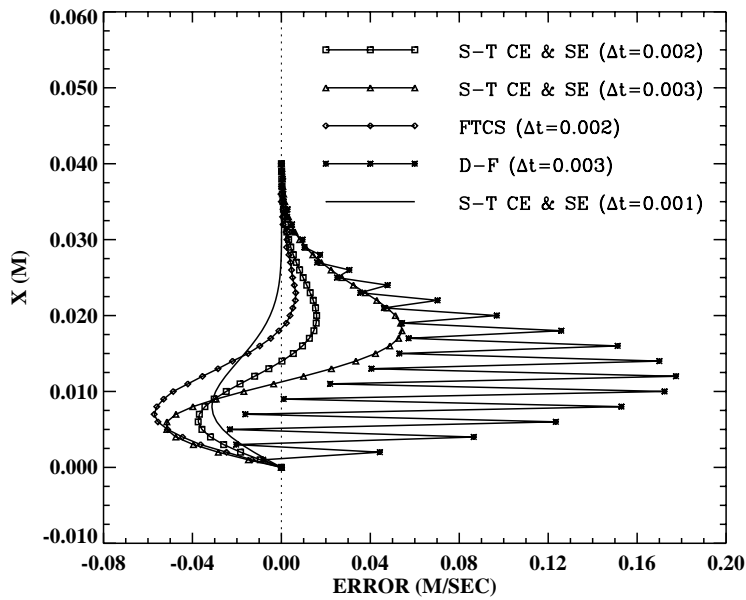


Figure 7: Error comparison of the μ scheme with other schemes at $t = 0.18\text{s}$ ($\Delta x = 0.001\text{m}$).

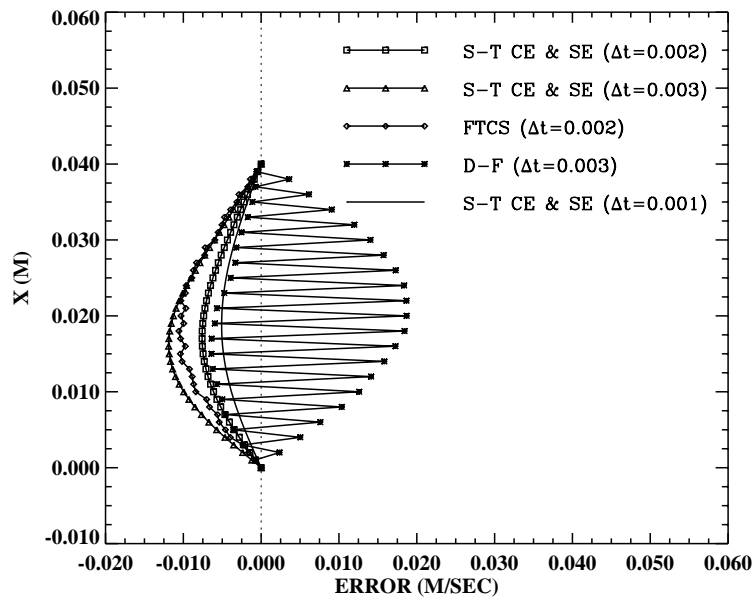


Figure 8: Error comparison of the μ scheme with other schemes at $t = 1.08s$ ($\Delta x = 0.001m$).

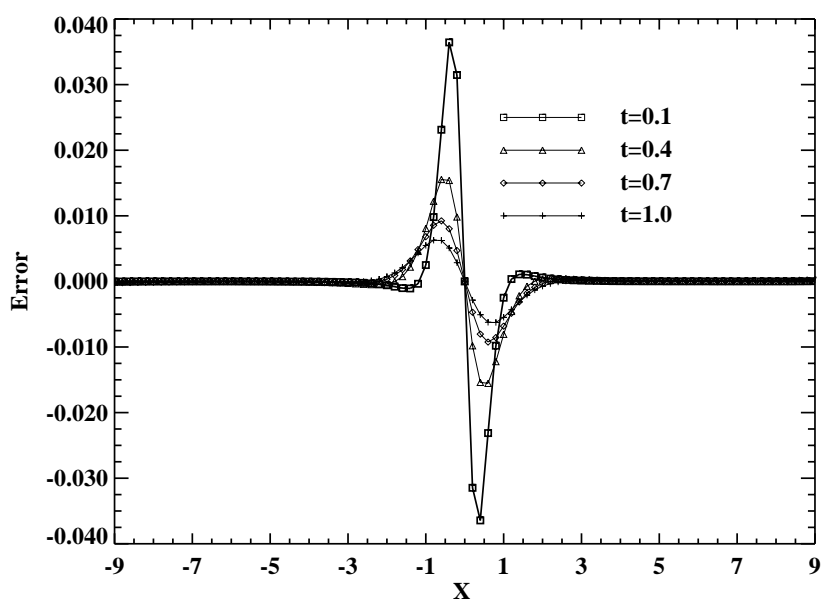
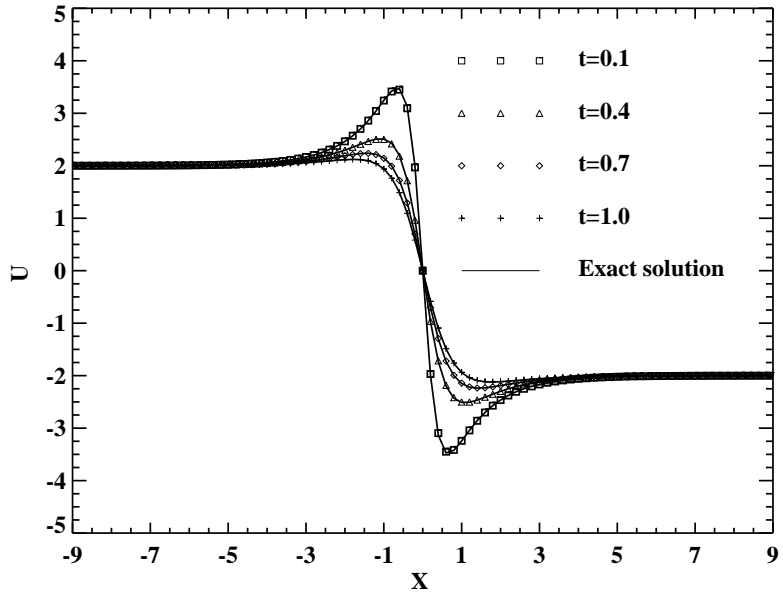


Figure 9: Solution of the viscous Burgers equation by the ν - μ scheme and the corresponding error distribution at different times ($\Delta x = 0.2, \Delta t = 0.01$).

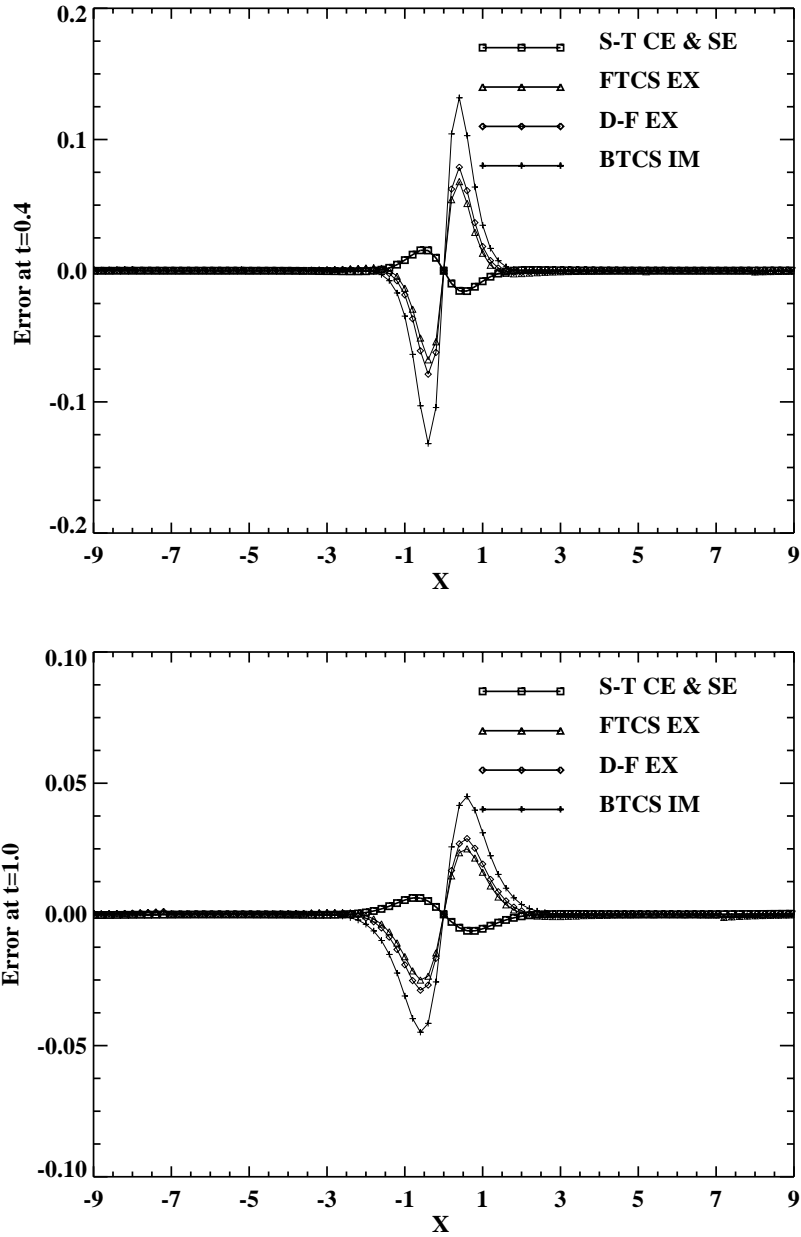


Figure 10: Error comparisons of the ν - μ scheme with other schemes ($\Delta x = 0.2, \Delta t = 0.01$).

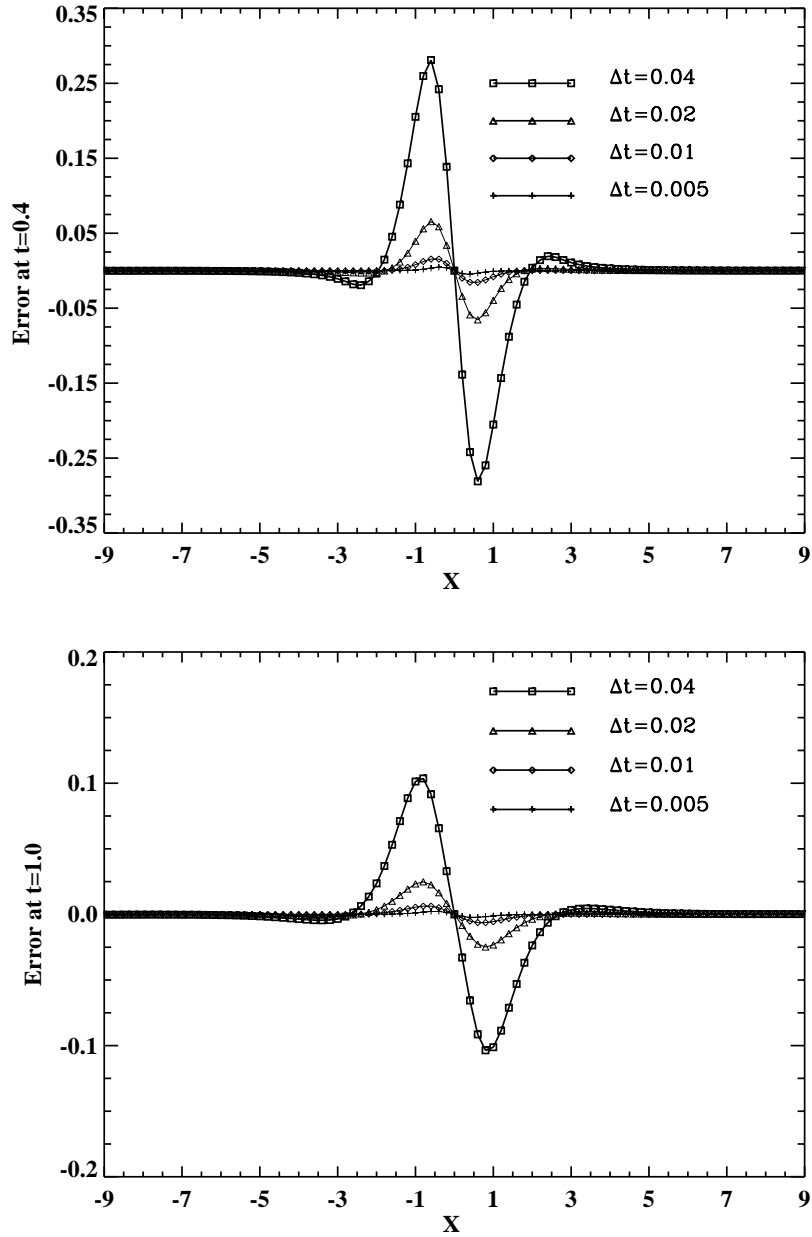


Figure 11: Error distribution of the ν - μ scheme for different time step sizes at $t = 0.4$ and 1.0 ($\Delta x = 0.2$).

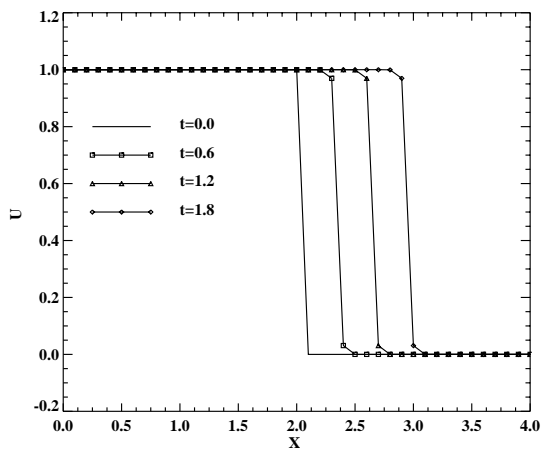


Figure 12: Solution of the inviscid Burgers equation at different times by the ν - ϵ scheme ($\Delta x = 0.1, \Delta t = 0.1$).

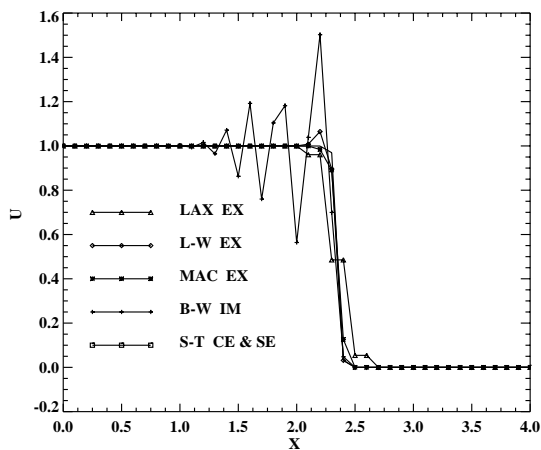


Figure 13: Comparison of the ν - ϵ scheme with other schemes at $t=0.6$ ($\Delta x = 0.1, \Delta t = 0.1$).

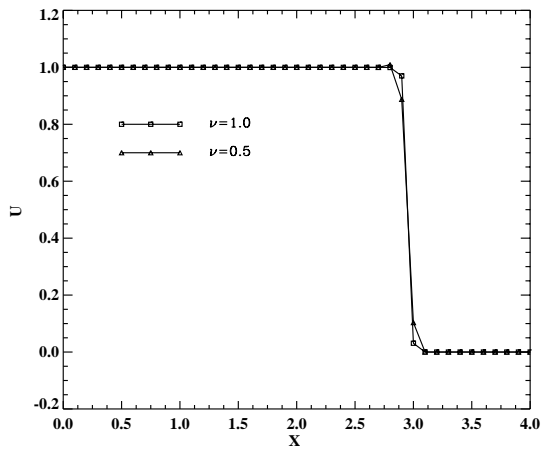


Figure 14: Effect of time step size on the accuracy of the ν - ϵ scheme ($\Delta x = 0.1$).

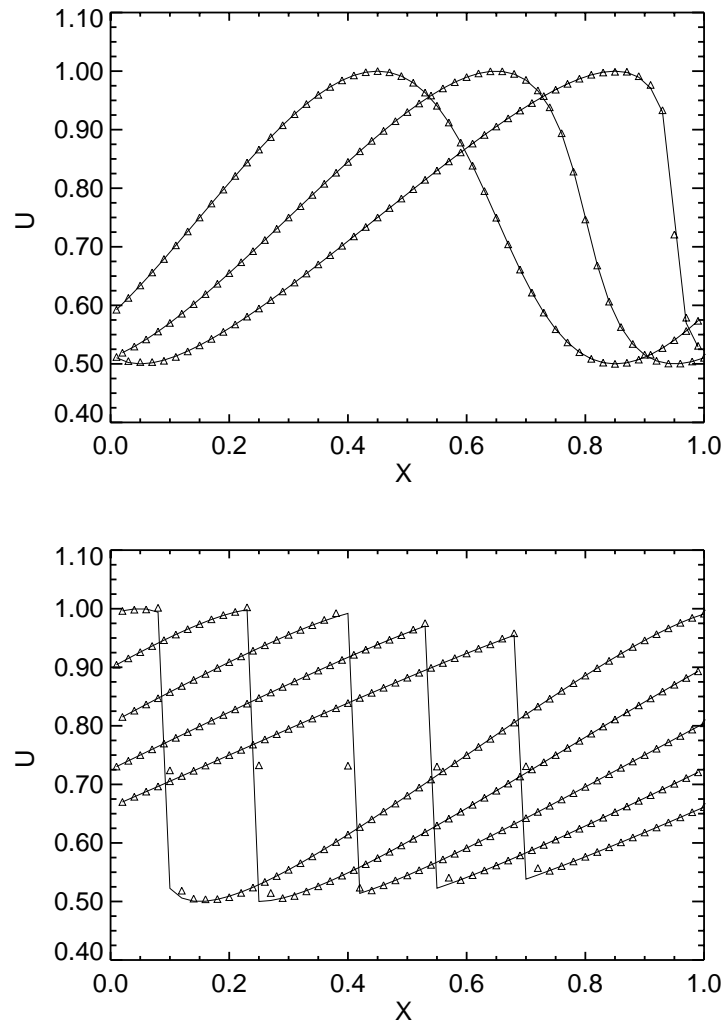


Figure 15: The CE/SE solutions(triangles) at $t = 0.2, 0.4, 0.6, 0.8, 1.0, 1.2, 1.4$ and 1.6 in comparison with the corresponding exact solution(solid lines).

REPORT DOCUMENTATION PAGE			<i>Form Approved</i> <i>OMB No. 0704-0188</i>	
Public reporting burden for this collection of information is estimated to average 1 hour per response, including the time for reviewing instructions, searching existing data sources, gathering and maintaining the data needed, and completing and reviewing the collection of information. Send comments regarding this burden estimate or any other aspect of this collection of information, including suggestions for reducing this burden, to Washington Headquarters Services, Directorate for Information Operations and Reports, 1215 Jefferson Davis Highway, Suite 1204, Arlington, VA 22202-4302, and to the Office of Management and Budget, Paperwork Reduction Project (0704-0188), Washington, DC 20503.				
1. AGENCY USE ONLY (Leave blank)		2. REPORT DATE April 1999	3. REPORT TYPE AND DATES COVERED Technical Memorandum	
4. TITLE AND SUBTITLE Application of the Space-Time Conservation Element and Solution Element Method to One-Dimensional Advection-Diffusion Problems			5. FUNDING NUMBERS WU-538-03-11-00	
6. AUTHOR(S) Xiao-Yen Wang, Chuen-Yen Chow, and Sin-Chung Chang				
7. PERFORMING ORGANIZATION NAME(S) AND ADDRESS(ES) National Aeronautics and Space Administration John H. Glenn Research Center at Lewis Field Cleveland, Ohio 44135-3191			8. PERFORMING ORGANIZATION REPORT NUMBER E-11624	
9. SPONSORING/MONITORING AGENCY NAME(S) AND ADDRESS(ES) National Aeronautics and Space Administration Washington, DC 20546-0001			10. SPONSORING/MONITORING AGENCY REPORT NUMBER NASA TM-1999-209068	
11. SUPPLEMENTARY NOTES Xiao-Yen Wang, Taitech, Inc., 2372 Lakeview Drive, Suite H, Beavercreek, Ohio 45431 (work funded under NASA Contract NAS3-97186); Chuen-Yen Chow, Department of Aerospace Engineering Sciences, University of Colorado at Boulder, Boulder, Colorado 80309; and Sin-Chung Chang, NASA Glenn Research Center. Responsible person, Sin-Chung Chang, organization code 5880, (216) 433-5874.				
12a. DISTRIBUTION/AVAILABILITY STATEMENT Unclassified - Unlimited Subject Categories: 34 and 64 This publication is available from the NASA Center for AeroSpace Information, (301) 621-0390.			12b. DISTRIBUTION CODE	
13. ABSTRACT (Maximum 200 words) Test problems are used to examine the performance of several one-dimensional numerical schemes based on the space-time conservation and solution element (CE/SE) method. Investigated in this paper are the CE/SE schemes constructed previously for solving the linear unsteady advection-diffusion equation and the schemes derived here for solving the nonlinear viscous and inviscid Burgers equations. In comparison with the numerical solutions obtained using several traditional finite-difference schemes with similar accuracy, the CE/SE solutions display much lower numerical dissipation and dispersion errors.				
14. SUBJECT TERMS CE/SE method; Advection-diffusion problems			15. NUMBER OF PAGES 29	
			16. PRICE CODE A03	
17. SECURITY CLASSIFICATION OF REPORT Unclassified	18. SECURITY CLASSIFICATION OF THIS PAGE Unclassified	19. SECURITY CLASSIFICATION OF ABSTRACT Unclassified	20. LIMITATION OF ABSTRACT	